Pacific Northwest
NATIONAL LABORATORY

PNNL-31459

Resiliency of Polycrystalline Diamond Bearings Exposed to Marine Environments

6/30/21

Nolann Williams James McVey Robert Jeters

U.S. DEPARTMENT OF ENERGY

Prepared for the U.S. Department of Energy
Under contract DE-AC05-76RL01830

DISCLAIMER

PACIFIC NORTHWEST NATIONAL LABORATORY
operated by
BATTELLE
for the
UNITED STATES DEPARTMENT OF ENERGY
under Contract DE-AC05-76RL01830

Printed in the United States of America

Available to DOE and DOE contractors from the
Office of Scientific and Technical Information,
P.O. Box 62, Oak Ridge, TN 37831-0062;
ph: (865) 576-8401
fax: (865) 576-5728
email: reports@adonis.osti.gov

Available to the public from the National Technical Information Service
5301 Shawnee Rd., Alexandria, VA 22312
ph: (800) 553-NTIS (6847)
email: orders@ntis.gov <https://www.ntis.gov/about>
Online ordering: http://www.ntis.gov

PNNL-31459

Resiliency of Polycrystalline Diamond Bearings Exposed to Marine Environments

6/30/21

Nolann Williams James McVey
Robert Jeters

Prepared for
the U.S. Department of Energy
Under Contract DE-AC05-76RL01830

Pacific Northwest National Laboratory
Richland, Washington 99352

Contents

Figures

Tables

1.0 Executive Summary

Marine energy efforts are increasingly focused on remote locations where traditional grid-tied systems are not practical. Seals and bearings in marine energy generators are a common source of failures, accounting for up to 25% failure rate per year. Polycrystalline diamond (PCD) bearings are composed of one of the most durable substances known to humankind and have been successfully tested in laboratory conditions for marine use. PCD bearings can be used to construct flooded marine energy generators that do not have seals, resulting in reduced maintenance while increased reliability for marine energy systems. PNNL built a bearing test stand to mimic conditions found in cross-flow turbines being built by researchers at the Applied Physics Laboratory at University of Washington. We exposed steel and PCD bearings in the bearing test stand to Arctic water temperatures (-2.4°C), fostering ice formation around bearing surfaces while monitoring bearing health for ~1,000 hours. While the steel bearings failed at the 990 hour mark, the PCD bearing showed virtually no signs of wear beyond characteristic self-polishing of bearing surfaces. The PCD bearing did not change weight appreciably, and while ice formation impacted bearing function when present, the coefficient of friction (CoF) of the bearings was approximately 0.05 without ice. PCD bearings present an opportunity for rugged marine power generation in flooded marine energy generators.

2.0 Introduction & Background

Marine Hydrokinetic (MHK) efforts are focusing increasingly on deployment to remote locations where traditional grid-tied systems do not reach or are not practical. These areas include Arctic research systems, which are distributed along the coast and used to monitor meteorology, water quality and climate change (Proshutinsky, Plueddemann, and Krishfield 2004). While the energy needs of these systems are modest, they require vessels to service them with fuel or batteries on a regular interval at high cost given their distance from service facilities. These locations are also seasonally inaccessible depending on ice and weather conditions, and a failure in the depths of winter will leave a system inoperable until the next spring. In addition to scientific endeavors in the Arctic, remote Alaskan communities are interested in renewable energy sources to potentially reduce the cost of energy and provided diverse and redundant energy sources (Robertson, Bekker, and Buckham 2020). Arctic energy systems provide for community energy needs and are essential to the safety and survival of the inhabitants. This necessitates reliable systems that can survive for extended deployment times with minimal maintenance and survive saltwater: a corrosive, abrasive, bioactive medium. Tidal and river based turbines are energy sources being evaluated for Arctic use as they can provide a consistent source of energy (Johnson and Pride 2010). The temperatures in Arctic water are low, consistently around -2°C or lower depending on the salinity, which can range from 0 to 45 g/kg. Much of the coast is covered in ice for 9 months of the year and turbines may be exposed to low temperatures and ice in the water depending on depth and location. Small scale turbines have components that are prone to failure in harsh marine conditions including seals, bearings, gearboxes and electric motors (Ewing et al. 2020). Bearings and seals fail more often than others due to the environment and high oscillatory loading (Wood et al. 2010). Recent research on direct drive generators provides a possible solution, as these generators do not need seals, gearboxes or electric motors (Janon, Sangounsak, and Sriwannarat 2020).

2.1 Tidal turbine seal failures

Statistical analysis of tidal turbines reliability indicates that the least reliable components are seals, which for power take-off subsystems have essentially a 25% chance of failure per year (Ewing et al. 2020). While the main failure point is in the seals, this is not the direct cause of tidal turbine failure, but simply the first step in a sequence. Seal failure allows seawater to contaminate the lubricant oil of the steel main bearing and associated moving parts, which degrades them to the point of failure. Repair is then not just replacement of a seal 0-ring, but potentially many parts damaged by seawater in the lubricant. If a generator bearings can operate in seawater and there is no internal gearing, such as in flux generators, then the seal can be removed from the system entirely.

2.2 Flooded generators

Flooded generators are filled with water and have no air or oil filled compartments requiring seals to exclude seawater. One common flooded design is a direct drive flux generator, which uses rare earth magnets on a disc that rotates on flooded bearings. The magnets are separated by a narrow gap filled with seawater from stationary coils of wire (armature) which produce power when the magnets rotate next to them. This removes all seals, gearboxes, and associated mechanical interfaces (Janon, Sangounsak, and Sriwannarat 2020). Recent research on direct drive flooded generators suggest they would be much more reliable than

alternatives, though direct drive generators require rare earth elements and bearings that can tolerate seawater.

2.3 PCD bearings

There are various types of bearings comprised of metals, ceramics, and composites that can be used in seawater. The most robust are polycrystalline diamond (PCD) bearings, a commercial newcomer. PCD bearings use sintered diamonds in a structured matrix that results in a durable bearing interface of diamond against diamond, with the two diamond facets layered on durable tungsten carbide shafts. The two diamond faces when first used have a brief period of higher friction while they self-polish smooth for a perfect mating (Knuteson, Sexton, and Cooley 2011). This self-polishing action makes these bearings forgiving in alignment as they will polish themselves smooth should alignment of the bearing change. Commercial offerings are available in many sizes and thrust, axial and tapered configurations that can be customized for a variety of generator topologies (1). PCD bearings have been used in the oil industry, where they are

Figure 1. US Synthetic PCD bearings are available in thrust, radial and tapered (not shown) configurations

used in drilling rigs to tunnel down through rock, using sand as a lubricant (Cooley, Khonsari, and Lingwall 2012). Marine use offers a gentler environment due to water's lubricating and heat-sinking capacity. PCD bearings have low coefficients of friction for sliding-type bearings, as evidenced by their use in industrial applications, though they are not as efficient as ball or roller bearings. PCD bearings have been tested for performance and reliability under laboratory conditions with synthetic seawater and various lubricants; however, data is limited for use in marine environments (Bromaghin et al. 2014). One of the greatest drawbacks to PCD bearings is their cost, which is approximately 80 times that of steel bearings of equivalent size (T. Kolste at US Synthetic, personal communication, April 2020). This factor may make PCD bearings ill-suited for cost efficient applications; on the other hand, many marine systems require robust components that could benefit from flooded generators with reduced maintenance costs (Wani, Dong, and Polinder 2020). While the bearing may be expensive, the removal of most moving mechanical parts will have a commensurate reduction in price from the absence of these systems while dramatically increasing reliability. Elimination of seals alone would increase reliability of some marine generators by ~400% and reduce maintenance costs and downtime..

3.0 Methods

Core methodology for the study is split between construction of a bearing test stand and experimentation. Each is described below.

3.1 Bearing test stand

Our work on PCD bearings focused on use cases for flooded bearing systems. Staff at the University of Washington Applied Physics Laboratory (APL) were consulted on a scale model cross-flow tidal turbine scheduled to be deployed at PNNL's Marine and Coastal Research Laboratory (MCRL) (P. Gibbs, personal communication, February 2020). The bearings in the APL turbine model are lubricated steel bearings in a sealed housing. A system diagram, Fig. 2, with known forces was used to guide the construction of a scale model PCD bearing test stand for submerging steel and PCD bearings in seawater under Arctic water temperatures while measuring bearing reaction torque and applied lateral side load. The bearing's outer race sat

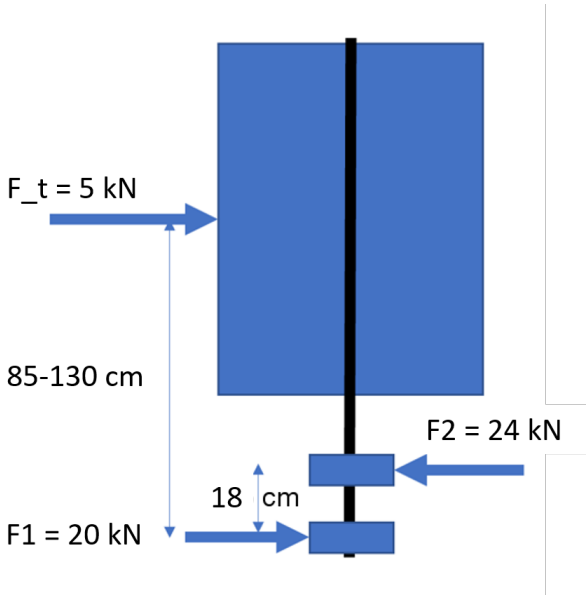

Figure 2. APL use case force diagram for a scale model cross flow turbine

within a static housing that was rigidly mounted to the base of support structure, with the bearing held in place by a retaining ring (Fig. 3). The bearing housing remained unsealed and allows full access by seawater as a lubricant to bearing surfaces. The bearing's inner race was mounted to a shaft, which in turn ran directly up to a gearmotor set to drive the shaft at 120 rpm. The gearmotor sat within a module rigidly mounted to the active flange of a torque cell, with the centerline of the shaft aligned with that of the motor drive and torque cell. The torque cell's inactive flange was rigidly mounted to the test structure, with the capability to adjust the position of the torque module vertically. The test structure itself was mounted on rails running across the test tank rim. The bearings were preloaded by applying a 120 N weight to the top of the torque cell module before fastening it in place. The rotating shaft (Fig. 4- Green) holds the inner PCD race against the outer (Fig. 4- Cyan) while lateral force was applied to the bearing via a slot machined through one half of the housing and was created by compressing a shaft (Fig. 4- Purple) between the bearing and an aluminum plate, incorporating a button load cell to

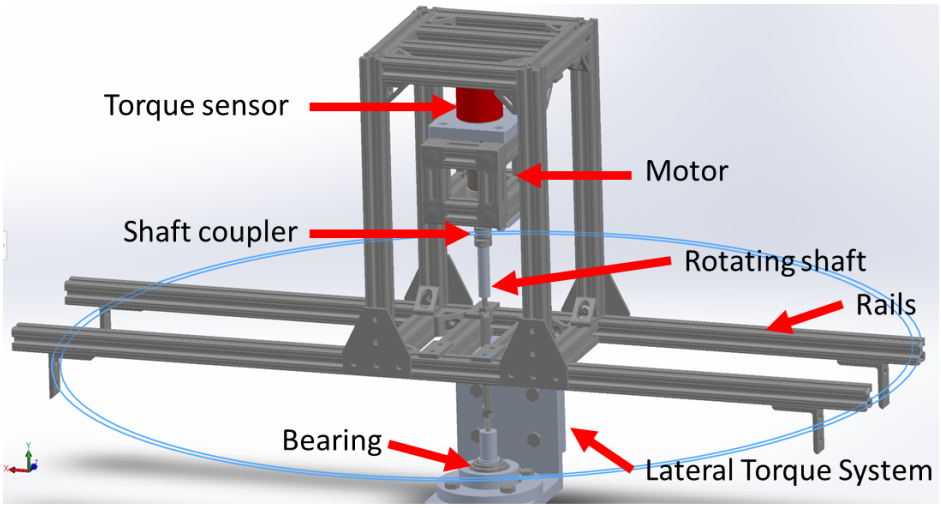

Figure 3. Bearing test stand design (left). Force is transmitted from the frame down through the torque sensor, motor, shaft coupler to the bearing itself

measure force (Fig. 4- Red). The coefficient of friction (CoF) is calculated by measuring the torque on the rotating shaft while a button load cell measures the side load. The friction

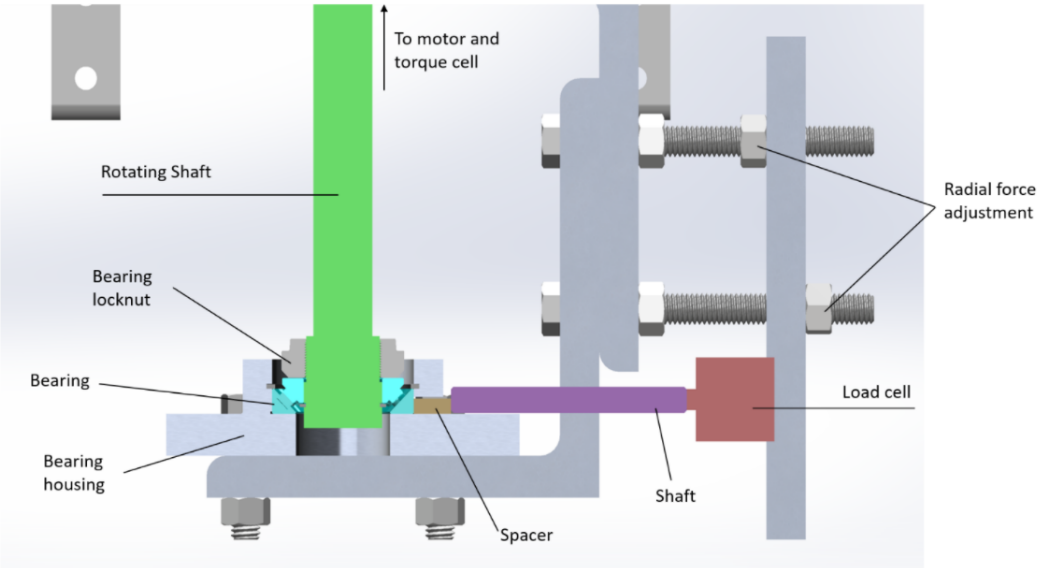

Figure 4. Close up of the bearing test stands lower assembly

coefficient of the bearing can be found from the applied side load and reaction torque by

$$F_{Friction} = \mu * F_{Normal}$$

Where F_{Normal} is the sum of the radial forces of the applied side load and pre-load, $F_{Friction}$ is calculated from the reaction torque divided by the bearing contact radius, and μ is the friction coefficient. With the motor running, any resistance/reaction from the bearing is transmitted up to and recorded by the torque cell. Because both bearings have taper angles (15 and 45 deg for steel and PCD, respectively), the normal force of the force equation is equivalent to the sum of

the radial forces due to the pre- and side-loading. To determine the magnitude of the side-load, first, steel tapered-roller bearings' maximum static radial loads were compared to the same bearings' shaft diameters, shown in Figure 5. Knowing the approximate radial load of APL's 4"

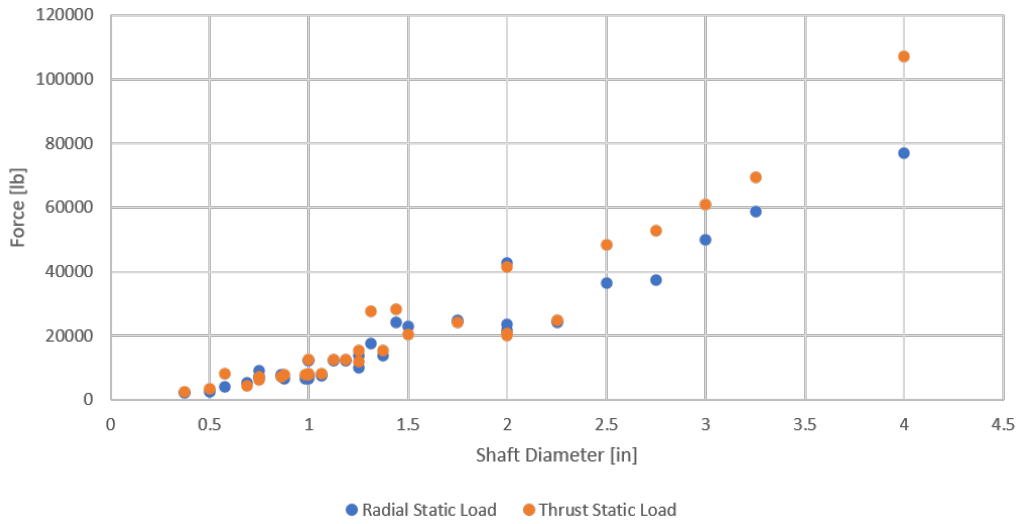

Figure 5. Tapered roller bearing maximum loads as listed on McMaster-Carr

bearing (F2 in Fig. 2) and the max load – shaft diameter relationship (Fig. 5), the approximate load to apply to the equivalent 1" bearing came out to 2.7 kN.

A 1" inner diameter (ID) bearing (Timkin L44643) was used for multiple system validation tests, and a PCD bearing with a 1" ID was provided by US Synthetic (a ChampionX Company) to compare against. The bearings were rotated by a Pololu #4694 metal gearmotor with helical pinion encoder driven by a RoboClaw 2X7A motor controller set to 120 rotations per minute.

3.2 Measurements

A Futek model TFF400 torque sensor with a 1,000 in-oz limit with amplifier set to 10.4 mV/in-oz was used to measure torque on the bearings and a LC304-3k miniature button compression load cell amplified to 7.1 mV/lb was used to measure side load. These were both fed into A1A-22B Anyload amplifiers coupled to a MX1105 Onset Datalogger logging at five second intervals which was analyzed in one-minute intervals (Fig. 6). Verification of the manufacturer's calibration of the torque sensor was performed by attaching a ring to the aluminum motor cage as seen in the upper portion of Fig. 3, 67 mm off the centerline of the shaft. A line was attached to this ring and run over a ball bearing mounted to a horizontal shaft clamped to the aluminum struts of the frame. The line's force to the pin bearing was perpendicular to the ring/shaft angle to result in a known torque. The line ran down to hanging weights of known values which were used to calibrate the output. The button load cell calibration was verified by placing a range of weights onto the button and calibrating off the amplified voltage measured.

3.3 Arctic laboratory & testing

Bearing durability tests were performed at the PNNL-MCRL Arctic simulation lab, where each bearing was subjected to approximately 1,000 hours of exposure to seawater with at least 700

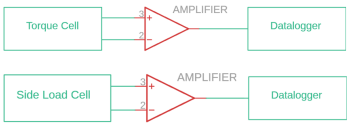

Figure 6. Torque (top) and button load cell (bottom) force sensor processing and datalogging electronics

hours at 120 rpm rotation in unfiltered seawater at an average temperature of -2.4°C, while logging bearing torque and side load. Steel and PCD bearings were weighed and photographed before installation into the bearing test stand. The test tank was filled until bearings were submerged under approximately 5 cm of seawater. A steel tapered-roller bearing served as a control during the first phase of testing, resulting in a baseline. Subsequent examination of a tapered PCD bearing was compared to the baseline to quantify wear as a function of exposure to raw seawater and freezing conditions, determine performance gains and make future recommendations. Temperature was logged from a TEWA TT0P-10KC3-T105-1500 Thermistor in series with a 0.1% precision 10k resistor being fed into a Landt CT3001D tester with a AT2016A auxiliary voltage monitoring system. The rails of the bearing test stand were attached to the sides of a 36” x 36” cylindrical fiberglass tank with c-clamps and 1/8’ neoprene strips between the rails and tank to reduce vibration (Fig. 7).

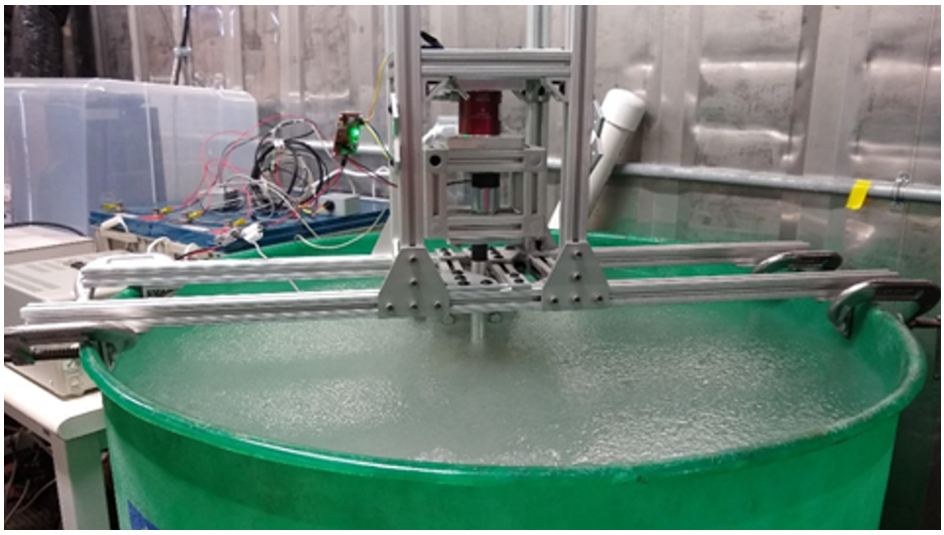

Figure 7. Bearing test stand in Arctic Laboratory with grease ice at surface

3.4 Post immersion processing

The bearings were removed following testing for photographs and weighing. PCD bearings were then subjected to a brief acid pickling process to remove aluminum oxide from our test stand that covered the surfaces of the bearings. The pickling acid was composed of 20% nitric and 2% chloric acid by volume at 16°C for 15 minutes with periodic agitation. Following the pickling, the bearings were rinsed in de-ionized water for 5 minutes and then dried on a hot plate set to 100°C for 2 minutes before weighing and follow-on photographs.

4.0 Results

4.1 Steel Bearing

Figure 8. New steel tapered roller bearings (left) and after 1000 hours seawater exposure (right). Orientation is the same for both pictures

The steel control bearings showed significant signs of corrosion after 1,000 hours submerged. Multiple regions of iron oxide buildup indicate seawater was oxidizing the bearing inner and outer races as well as the rollers (Fig. 8). Instances of galling on the races are visible as vertical abrasions in the metal in a distinct repeating pattern of the same spacing as the tapered rollers themselves. This suggests that when the rollers abraded the surface, they followed a consistent pattern on the races and not at random across the surface. Side load did not stay constant over the course of the testing (Fig. 9). The side load constantly decreased around 5 lb/day until it suddenly dropped precipitously to zero 5 weeks into testing. The steel bearing's reaction torque remained constant until the side load dropped and torque increased exponentially, the reason for which is unknown. The steel bearings have a much higher CoF than published values, most likely due to immersion in raw seawater, ice formation, and lack of proper lubrication. They held up for 990 hours before failure. Examination of the bearings themselves showed corrosion products on the rollers and races, though the bearing could be made to spin freely with application of sufficient force. Regardless, the bearings would quickly seize up again after several low friction rotations.

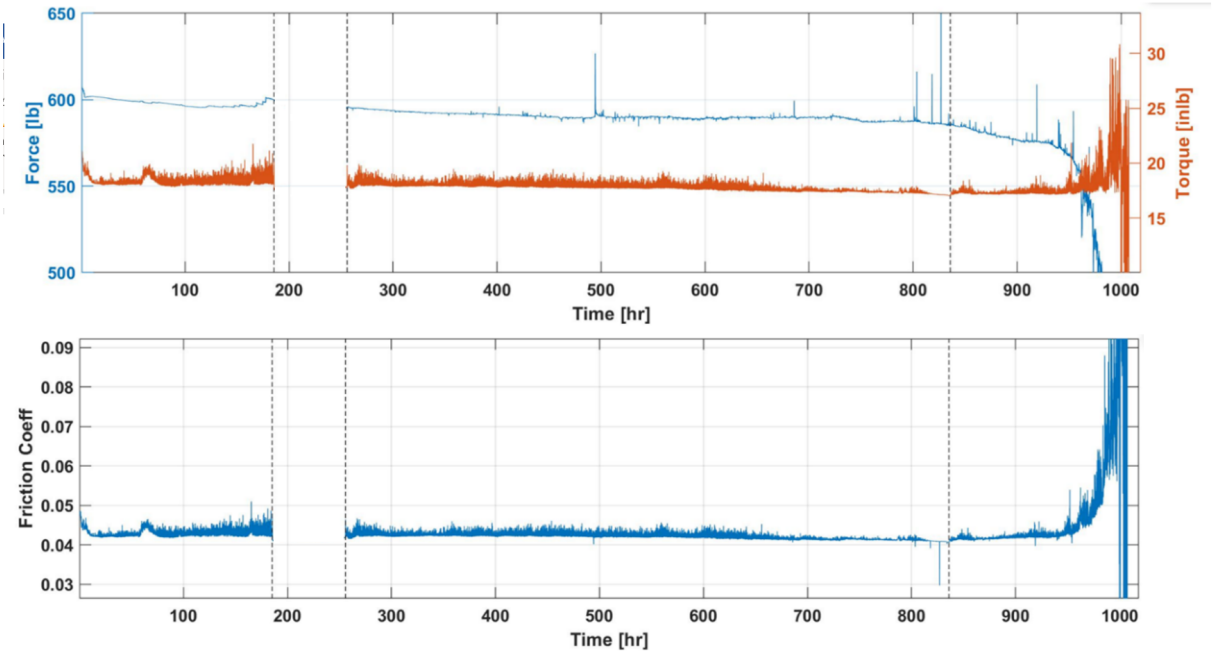

Figure 9. Steel bearing lateral force and reaction torque vs time. The top graph is the lateral force (blue) and reaction torque (red) while the bottom graph is of the coefficient of friction for the steel bearings

4.2 PCD Bearing

The bearings on arrival were free of any observable defect such as hairline cracks or tarnishing (Fig. 10- left). The brazing used to adhere the PCD inserts into the duplex steel matrix did not show any inclusions or discontinuities. After testing, the bearing's inner race showed a ring of iron oxide from the iron retaining ring helping secure the race to the shaft, and while white aluminum corrosion covered the majority of the bearing surface, no corrosion of the brazing or steel matrix was evident (Fig. 10- middle). The aluminum corrosion from our test stand sloughing off and coating everything was likely aluminum oxide, the crystalline form of which is corundum, which has a Mohs hardness of 9. Aluminum oxide is used as a commercial abrasive as it will scratch virtually all other minerals except diamond. After acid washing, the bearings looked virtually identical to their pre-test state with the exception of the polished wear patterns where the bearing pads were in contact (Fig. 10- right).

Stereomicroscope examination of the PCD bearing wear surfaces, as seen in Figure 11 show no degradation of any PCD bearing surface, though some forms of corrosion would have been removed by the pickling acid dip on the brazing or matrix. The wear pattern on the inner race was evenly spread across all bearing facets in the same approximate location indicating consistent spreading of load and high-quality manufacturing.

The weight of both bearings increased by approximately 15 mg during testing; however, after the acid wash to remove sloughed off corrosion from our test stand, the before and after weights were virtually identical (Table 1). After averaging, the friction coefficient was calculated based on Equation 1, and the timeseries data (force, torque, friction coefficient) were partitioned into sections based on the variance of the friction coefficient timeseries. The variance of the torque data changes periodically, which were divided into sections shown in Figure 9. For each

Figure 10. Inner race (top) and outer race (bottom) photographs. New PCD bearings (left), after running for 1,000 hours (middle), and after an acid wash (right). All pictures are taken from the same orientation.

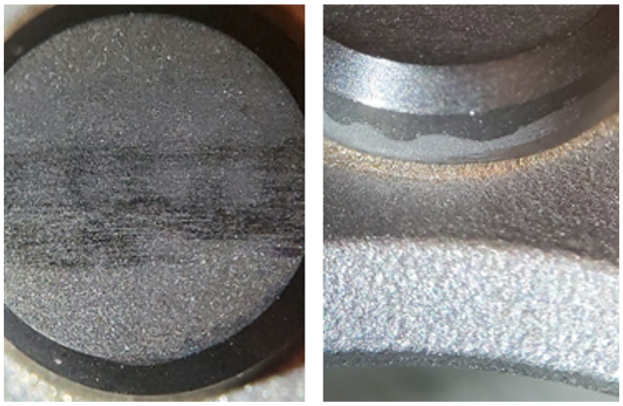

Figure 11. Following the acid pickling the surface of the PCD bearing diamond facet (left) and the brazing (right) show minimal wear except for self-polishing action

of these periods, the Pearson's correlation coefficient between the side force and torque data is calculated and is shown in Table 2. Sections in Table 2 labeled N/A are periods of time when the motor is not running. Because the relationship between the side load and reaction torque is linear, in ideal conditions this coefficient should be unity. When the coefficient is low, it implies there are other independent variables affecting the reaction torque, e.g. ice stress or particles between the contact bearing surfaces. The friction coefficient of the PCD bearing begins at 0.073 and decreases to 0.06 in the first two days, after which it begins increasing with the side load (Fig. 12). It varies considerably, as does the timeseries' variance, between the start of the test through the end of section 3, where there appears to be an equilibrium, but continues to undergo periodic shifts to a new equilibrium around a friction coefficient of 0.05. Ice froze the bearing immobile after section labeled #5, and the correlation drops nearly to zero after this point in testing. Sections of figure 12 have no data as the bearing was not running during this time period but remaining static in the tanks.

Table 1. Weights of PCD bearing before testing, after removal, and after a 15 minute acid dip to remove corrosion

	Initial (g)	After testing (g)	After acid wash (g)	Difference (mg)
Inner race	37.1608	37.1744	37.1598	-1
Outer race	39.9297	39.9435	39.9296	-0.1

Table 2. Side Load to Reaction Torque Correlation Coefficient

Bearing Section	1	2	3	4	5	6	7	8
Pearson's R	0.70	0.36	-0.63	0.77	0.0	N/A	0.18	0.08

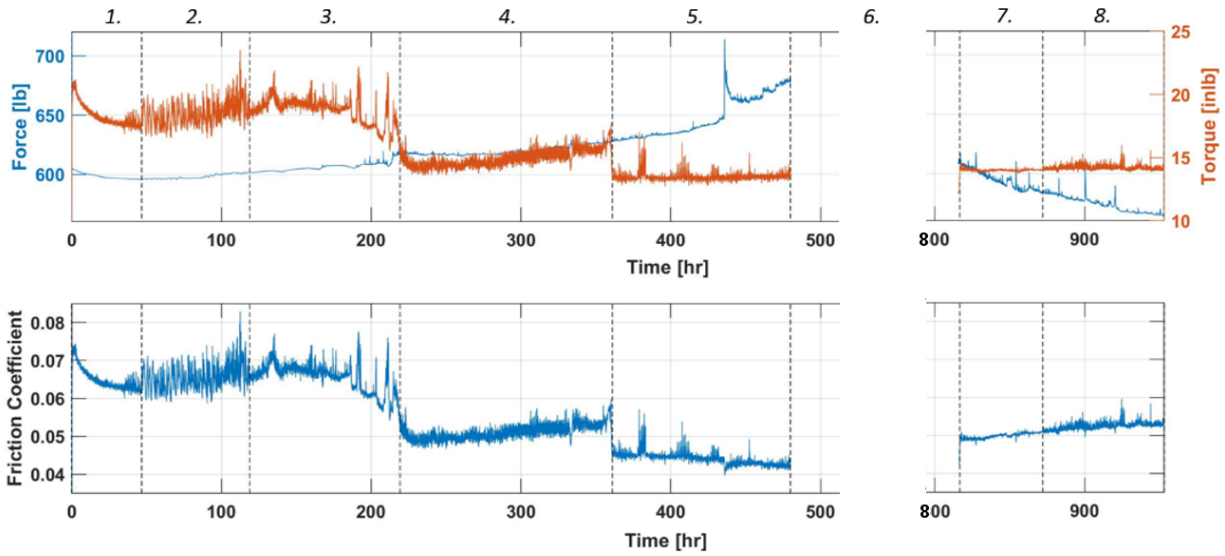

Figure 12. PCD Side force & reaction torque vs time

4.3 Ice State

Ambient conditions did not remain constant throughout the length of testing. Ice within the test tank underwent multiple freeze-thaw cycles as Arctic Lab temperatures changed due to power outages and external factors. Room-temperature seawater formed a frazil ice structure at the surface after the test began and continued to freeze until it reached a state of grease ice. When the temperature of the Arctic Lab was cycled (i.e. above and below freezing), grease ice made the transition into forming solid "ice pack", which froze 5-6 in of the surface layer down to the level of the bearings (Fig. 13). The bearings rotated in all ice conditions freely, though ice slurry would build up around the shaft over time. These changes in temperature continually altered the ice state within the tank, which induced external stresses on the test stand and altered loads on the bearing. At the end of section 5, ice stress locked up the shaft and burned out the fuse. The ice in the tank then had to be melted to free the shaft and bearing before restarting the motor.

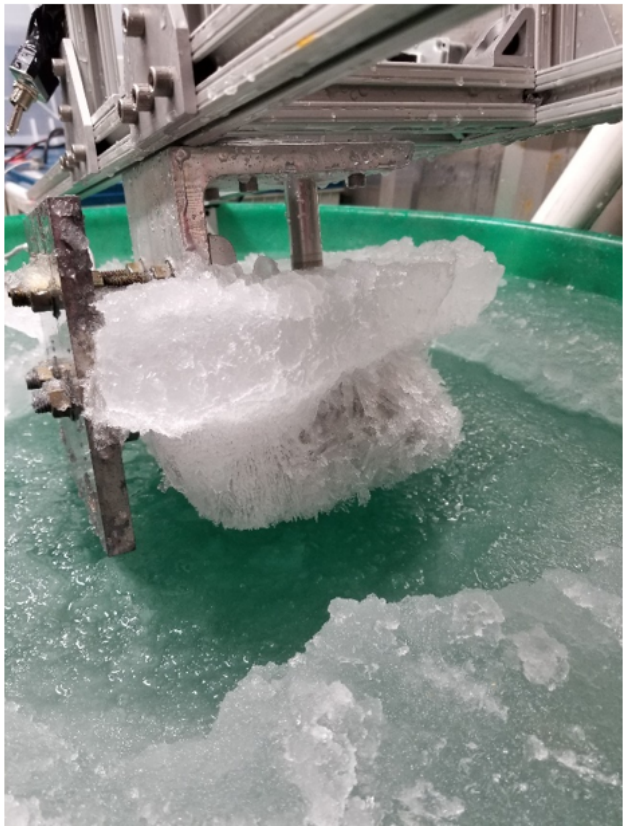

Figure 13. The PCD bearing after 450 hours of running with ice buildup in the bearing

5.0 Discussion

The testing performed on steel bearings underscores that they were never meant to be run in raw seawater without lubrication, let alone in ice. Steel bearing failure showed jumps in bearing CoF followed by a return to baseline as the bearings seized in their races momentarily before spinning freely again, most likely due to both ice stress and particles/corrosion on the races. The wholesale corrosion of all bearing races and rollers are a likely source of material to bind up the roller bearings and highlights the importance of clean lubricant. Real world applications are unlikely to see such gross damage, though seal failure will introduce microscopic droplets of seawater into the lubricant oil and cause similar but gradual degradation of exposed metal surfaces. The steel bearing's failure within 1,000 hours of testing highlights the abrasive nature of the testing, both for the seawater medium and freezing conditions. The PCD bearings supplied by US Synthetic performed well throughout testing in the Arctic Laboratory, despite being exposed to conditions worse than would be seen in most real-world applications. Tidal turbines are typically deployed in seawater environments at depths where the minimum temperature is bounded by the freezing temperature of seawater at -2.1°C (or less if higher salinity), and due to deployment depth should never see ice formation. The PCD bearings were subjected to freezing temperatures that converted surface seawater into a slurry of ice crystals. As this water froze, additional stresses were likely placed on all system components as the ice crystals grew and expanded in volume. Besides cold temperatures, the bearings were subjected to sediment from raw seawater and coated with a thin layer of aluminum corrosion similar to powdered sandpaper, likely increasing the friction of the wearing surfaces, though it had little evidence of surface corrosion like the steel bearing. Almost no degradation of the PCD bearing was noted by weight change, surface corrosion or bearing pad wear. The wear pattern of the bearings was not to the point where they would be considered broken in from self polishing action. This is likely the result of PCD bearing over-engineering, as the loads applied emulated steel bearings. The stability of the PCD bearings is promising for use in Arctic and marine conditions.

6.0 Conclusions

Remote MHK energy is of great interest to remote communities and research platforms due to the paucity of energy available and low reliability of existing renewable energy sources. Non-flooded generator designs are highly efficient and used for the majority of tidal turbines tested, but have common modes of failure. Flooded generators are largely theoretical at this time; however, proposed designs would removed the majority of failure modes documented for flooded designs. While there are a variety of materials (ceramic, plastic, engineered materials) available for use in flooded generators, PCD bearings are uniquely resilient in their resistance to degradation and ability to handle thermal loads. Testing in corrosive seawater with sediment loads and freezing conditions for 1,000 hours did not have any noticeable impact on bearing health beyond gentle wear patterns and minor weight reductions. While the cost of PCD bearings should be taken into account for marine systems, for those that require extreme durability, PCD bearings are recommended for further study in flooded generator designs.

References

Bromaghin, A., M. Ali, T. Ravens, T. Petersen, and J. Hoffman. 2014. "Experimental study of abrasion characteristics for critical sliding components for use in hydrokinetic devices." *Renewable Energy* 66:205–214. ISSN: 0960-1481. https://doi.org/https://doi.org/10.1016/j.renene.2013.11.069. https://www.sciencedirect.com/science/article/pii/S0960148113006575.

Cooley, Craig H., Michael M. Khonsari, and Brent Lingwall. 2012. *The Development of Open Water-lubricated Polycrystalline Diamond (PCD) Thrust Bearings for Use in Marine Hydrokinetic (MHK) Energy Machines.* University of Melbourne.

Ewing, Fraser J., Philipp R. Thies, Jonathan Shek, and Claudio Bittencourt Ferreira. 2020. "Probabilistic failure rate model of a tidal turbine pitch system." *Renewable Energy* 160:987–997. ISSN: 0960-1481. https://doi.org/https://doi.org/10.1016/j.renene.2020.06.142. https://www.sciencedirect.com/science/article/pii/S0960148120310648.

Janon, Akraphon, Krittattee Sangounsak, and Warat Sriwannarat. 2020. "Making a case for a Non-standard frequency axial-flux permanent-magnet generator in an ultra-low speed direct-drive hydrokinetic turbine system." *AIMS Energy* 8 (2): 156–168. https://doi.org/https://10.3934/energy.2020.2.156.

Johnson, J., and D. Pride. 2010. *River, Tidal, and Ocean Current Hydrokinetic Energy Technologies: Status and Future Opportunities in Alaska.* Alaska Energy Authority.

Knuteson, C.W., T.N. Sexton, and C.H. Cooley. 2011. "Wear-in behaviour of polycrystalline diamond thrust bearings." 18th International Conference on Wear of Materials, *Wear* 271 (9): 2106–2110. ISSN: 0043-1648. https://doi.org/https://doi.org/10.1016/j.wear.2010.12.059. https://www.sciencedirect.com/science/article/pii/S0043164811002304.

Proshutinsky, A., J. Plueddemann, and R. Krishfield. 2004. "Ice-Based Observatories: A strategy for improved understanding of the Arctic atmosphere-ice-ocean environment within the context of an Integrated Arctic Observing System."

Robertson, Bryson, Jessica Bekker, and Bradley Buckham. 2020. "Renewable integration for remote communities: Comparative allowable cost analyses for hydro, solar and wave energy." *Applied Energy* 264:114677. ISSN: 0306-2619. https://doi.org/https://doi.org/10.1016/j.apenergy.2020.114677. https://www.sciencedirect.com/science/article/pii/S0306261920301896.

Wani, Faisal, Jianning Dong, and Henk Polinder. 2020. *Tidal Turbine Generators, Advances in Modelling and Control of Wind and Hydrogenerators.* Intechopen. https://doi.org/https://10.5772/intechopen.90433.

Wood, Robert J.K., Abubakr S. Bahaj, Stephen R. Turnock, Ling Wang, and Martin-Halfdan Evans. 2010. "Tribological design constraints of marine renewable energy systems." *Philosophical Transactions of the Royal Society A: Mathematical, Physical and Engineering Sciences* 368:4807–4827. doi:10.1098/rsta.2010.0192.

Pacific Northwest National Laboratory

902 Battelle Boulevard
P.O. Box 999
Richland, WA 99352
1-888-375-PNNL (7675)

www.pnnl.gov